



Analysis of acupuncture principle on subjects using k Singular Value Decomposition

K.Thaiyalnayaki¹, Krishnasamy Kamala²

¹Svce, India, thaiyalnayaki@gmail.com

²Healer,M.D,Acu,Varma, India,thaiu_au@rediffmail.com

ABSTRACT

Promising fMRI(functional Magnetic Resonance Imaging) analysis methods have provided insight into the brain networks and brought reconciliation to acupuncture effects. In this present study , Ksvd(k Singular Value Decomposition) Technique is employed to identify the brain network involved in acupuncture activation for a old age shaky hand subject. Task analysis mostly employ 'seed voxel' method ,where a voxel or group of voxel's averaged time course from the seeding area is correlated with the time course of each voxel over the entire brain to generate connectivity maps . In Ksvd analysis , a dictionary is constructed and trained to identify the activated voxels of single subject . In this acupuncture analysis study, brain behavior after short stimuli , such as MA at acupoint LI 11,GB 34, identifies change with amygdale brain network for pain perception and pain modulation, sensory motor cortex for shaky hand were identified and these specific effect arise from the cooperation of brain regions engaged in Task and rest fMRI .

Key words : fMRI , Ksvd , MA , LI 11,GB 34,sensory motor cortex, pain perception.

1. INTRODUCTION

fMRI ,investigation on the hemodynamic BOLD effect, has come to dominate the brain mapping field due to its minimal invasiveness, no radiation exposure, good spatial resolution and wide availability. In previous decade an increasing number of studies applied fMRI to investigate acupuncture stimulation. Acupuncture is one of the most important therapeutic modalities in traditional Chinese medicine (TCM). It utilizes fine needles that may pierce through specific anatomical points (named 'acupoints') so that certain healing effects are produced[1]. Meta-analysis for verum acupuncture stimuli confirmed brain activity within many of the regions ,brain stem,cerebellum.[2]Acupuncture studies in fMRI did not quantify and explicitly distinguish subjects into de-qi and sharp pain based on needle sensations, which made striking discrepancies between results of different studies. What are the de-qi related BOLD responses, that is, are they dominated by activation or deactivation? What is the relationship between the de-qi related and the sharp pain related BOLD responses?The different regions were defined as regions of interest (ROIs) and correlated with the scores from the needling sensations.[3] Neuroimaging studies have shown that acupuncture stimulation

activates the brain regions, primary somatosensory cortex , secondary somatosensory cortex , anterior cingulate cortex insular cortex, prefrontal cortex, amygdala, hippocampus, periaqueductal gray and hypothalamus.[6]The comparisons between different resting states disclosed the discrepancies between the pre and post needling effects in the Brain[4].The canonical HRF is the basis of a parametric model that estimates changes in the fMRI blood oxygen level dependent (BOLD) signal. The major problem in the hypothesis-driven method is the nonadaptivity of the canonical HRF [7]. To overcome these drawbacks, a variety of data-driven methods have been suggested[8] including PCA, ICA. In this study , a manual acupuncture at acupoint LI 11,GB 34 for a shaky hand aged subject is analysed to identify the difference in activation in sensory motor cortex using Ksvd, a multivariate analysis method, as this method has the potential of exploring the effect of acupuncture on brain activities.

2. MATERIALS AND METHODS

In this fMRI experiment of single trial, slices of images are acquired for 110 scans , with each image consisting of roughly 200,000 voxels. Though a good number of these voxel consist solely of background noise and can be excluded from further analysis, the data that needs to be analyzed is staggering. The second author with in clinical practice for over 25 years, administered acupuncture manually. Stainless steel needles used for LI 11,GB 34 are 0.2 mm in diameter and 40 mm in length. The experiment is repeated twice for the same subject with rest fMRI in between and have 2 runs for comparison of analysis which facilitates population inference. The subjects eyes were closed,so they can't observe the procedures.

2.1 SUBJECT AND ACUPUNCTURE

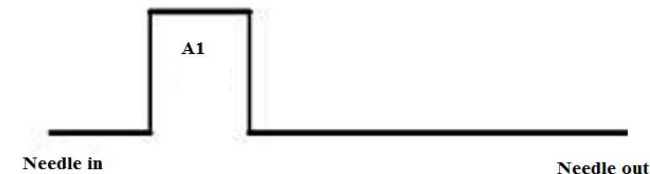


Figure:1Block run with acupuncture stimulation points and Rest fMRI.

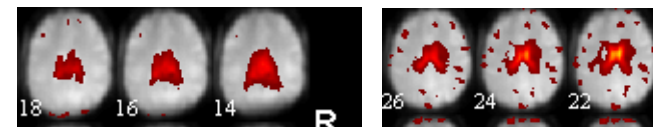


Figure 2:Activation reduced due to acupuncture in accupoint GB 34 and LI 11.Sagittal output is shown .

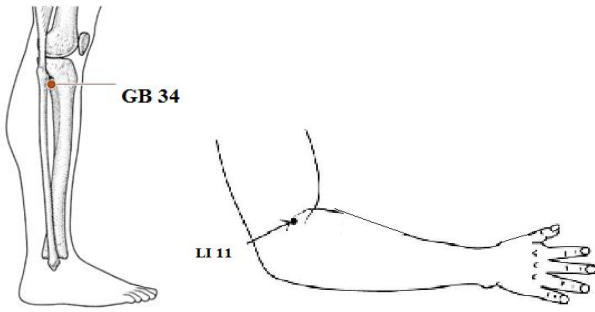


Figure 3:Acupoint GB 34 and LI 11 for improving the localization in sensory motor cortex.

Subjects were scanned in a 3.0 Tesla MR whole body Scanner. Functional images were collected in a sagittal orientation parallel to the AC-PC plane with 5 mm slice thickness using a single-shot gradient-recalled echo planar imaging (EPI) sequence. The EPI pulse sequence had the following parameters: TR = 1500 ms, TE is 40 ms, flip angle = 90 degree; matrix size = 64 × 64, FOV 240 × 240 mm², giving an in-plane resolution = 1.8 × 1.8 mm. The scan covered the entire brain . Structural scans were acquired using 3D MRI sequences with a voxel size of 1 mm³ for anatomical localization.

2.2 Sparse k SVD

The natural signals can be compactly expressed, or efficiently approximated, as a linear combination of prespecified atom signals, where the linear coefficients are sparse (i.e., most of them zero). Sparse coding approximates an input signal, Y, by a sparse linear combination of items from dictionary D. K- SVD algorithm is a powerful iterative algorithm for training sparse dictionaries. The K-SVD algorithm can find the dictionary D that yields sparse representations for a set of training examples.[9]Specifically, this problem can be mathematically described by

$$\min_{D,X} \{ \|Y - DX\|_F^2 \} \quad \text{Subject to } \forall i, \|x_i\|_0 \leq T_0 \quad (1)$$

Where Y is the data elements , X the coefficients of the signal. The K-SVD algorithm is a two step process: Sparse coding step, Code book update step. Exact determination of sparsest representations proves to be an NP-hard problem, approximate solutions are considered instead. The simplest ones are the Matching Pursuit (MP), the Orthogonal Matching Pursuit (OMP) algorithms. With estimated X, K-SVD puts only one column in the dictionary d_i and corresponding x_j, the jth row of X. This is solved using Single Value Decomposition (SVD)[8] .The columns of dictionary are sequentially changed and corresponding coefficients are updated.

2.3 Method of Optimal Direction (MOD) algorithm

This method closely follows the K-Means Algorithm. The sparse coding stage uses OMP algorithm .Assuming the coding for each example is known, the error is defined as

$$e_i = y_i - DX \quad (2)$$

Assuming X is fixed, an update to D such that the above error minimizes

$$D(n+1) = D(n) + \eta EX(n)T \quad (3)$$

Using infinitely many iteration and small η, leads to a steady state outcome and that is the MOD update matrix. MOD method assumes known coefficients at each iteration, and derives the best possible dictionary. After the dictionary learning with optimum k at each voxel, the non zero k atoms are used as the design matrix. Then F – map is calculated and degree of freedom should be imported to the SPM12 tool box to obtain the activation map for a given p- value.

3. INFERENCE AND DISCUSSION

Table 1: 110 acquisition arranged as columns against detrended voxels of whole brain.

		ACQUISITION												
		1	2	3	4	5	6	7	8	9	10	11	12	13
VOXEL	1	1	82.2515	82.4653	81.8371	77.2696	75.2351	74.4796	79.4647	79.2358	80.9912	78.9178	77.1285	73.7854
	2	1	139.9917	138.9332	134.4615	138.9899	138.9494	117.6304	123.9585	126.8447	124.2608	123.4614	123.2892	
	3	1	172.4408	178.5406	170.7201	164.2202	152.0621	150.1431	149.4925	153.7736	153.6070	155.8533	158.1413	156.1550
	4	1	188.9870	203.2423	194.1587	186.6657	182.3289	181.6894	179.4811	180.4493	177.9769	180.8539	182.8240	187.7543
	5	1	220.2983	215.5014	214.9326	211.4987	212.8435	211.2967	207.7710	205.8388	204.7955	200.0377	211.5402	216.2343
	6	1	178.4870	207.7801	176.2149	173.3010	174.2171	168.9310	170.6711	172.6132	171.0948	171.6667	166.3972	174.8467
	7	1	296.0002	286.5431	294.6693	288.4842	288.9788	283.9124	288.8715	294.5136	293.5052	291.8804	289.2347	293.4890
	8	1	301.4125	297.6292	301.6100	291.9595	293.9425	284.5192	296.3024	292.6385	293.9923	293.3623	287.8688	293.0419
	9	1	380.8670	382.0553	386.8342	381.9596	385.1557	349.5223	347.8221	348.6359	369.9795	363.9555	352.2220	357.0598
	10	1	127.0295	141.8865	131.6208	126.9971	127.8668	123.1328	115.2685	120.1262	128.6455	140.7465	138.9809	126.7016
	11	1	183.4683	191.1622	179.5888	180.0590	174.6770	174.9245	164.3077	183.7367	187.3820	189.1457	189.8455	177.7215
	12	1	147.5307	152.0016	144.6203	141.6582	136.9510	139.2129	137.2656	148.0711	148.8257	142.5763	132.3859	140.5957
	13	1	149.7963	155.9208	155.3244	151.0031	141.8645	141.7263	143.3379	149.2264	148.9201	144.0695	141.7462	142.2296
	14	1	132.8478	200.7388	194.0103	186.9919	171.2538	173.5138	179.4663	184.7438	181.3534	172.8466	154.6588	174.6396
	15	1	238.8628	249.2507	236.9001	229.2358	211.3302	210.5233	216.4396	213.1265	215.4690	215.4155	213.0715	
	16	1	282.4656	286.2364	271.9078	267.0664	258.3273	261.6150	257.5315	257.8736	252.0272	254.5108	255.1354	259.1843
	17	1	366.1744	302.3038	303.3136	295.1121	286.4719	286.9446	291.2440	290.3444	289.6250	294.6461	289.7977	299.1534
	18	1	301.4662	302.3679	302.2669	286.9044	292.4668	291.9789	288.6885	287.9447	288.8952	302.1212	287.4672	
	19	1	366.7707	356.9576	366.2979	360.5034	360.8996	354.0304	360.4198	367.6423	370.0008	365.0981	362.1468	362.6197
	20	1	174.8267	170.2787	173.2672	164.1650	166.6650	155.1937	160.4729	163.1199	168.0050	163.5324	155.2193	157.8817

Table 2: K-10 , Iteration =30, Sparse dictionary learning using Ksvd Algorithm.

Sparse matrix(X)		Dictionary (D)						
		1	2	3	4	5	6	7
1	0	-0.2468	-0.2074	-0.3017	-0.0726	-0.3853	-0.5369	
2	0.4112	0.5757	0.3064	0.2122	0	0	0	
3	-0.1801	0	0	0	0	0.4237	0.5293	
4	0.3004	0.1103	0	0.1838	0.1538	0	0	
5	0	0	0	0	0	0	0.0264	
6	0	0.2718	0.2725	0	0.1531	0.1356	0.1627	
7	0	0	0.1225	0.3707	0.3401	0.3210	0.0792	
8	-0.2570	0	0	-0.3372	-0.3424	-0.2169	0	
9	-0.1263	-0.4681	-0.2880	0	0	0	0	
10	-0.6087	-0.8751	-0.9097	-0.9862	-0.8821	-0.8367	-0.8545	

Dictionary (D)		1	2	3	4	5	6	7	8	9
1	0.0022	0.0012	0.0012	0.0012	0.0012	0.0012	0.0012	0.0012	0.0012	0.0012
2	0.0019	0.0019	0.0019	0.0019	0.0019	0.0019	0.0019	0.0019	0.0019	0.0019
3	0.0041	0.0042	0.0042	0.0041	0.0041	0.0041	0.0041	0.0041	0.0041	0.0041
4	0.0063	0.0063	0.0063	0.0062	0.0062	0.0062	0.0062	0.0062	0.0062	0.0062
5	0.0069	0.0069	0.0069	0.0068	0.0068	0.0068	0.0068	0.0068	0.0068	0.0068
6	0.0066	0.0066	0.0066	0.0066	0.0066	0.0066	0.0066	0.0066	0.0066	0.0066
7	0.0067	0.0067	0.0067	0.0067	0.0067	0.0067	0.0067	0.0067	0.0067	0.0067
8	0.0065	0.0065	0.0065	0.0065	0.0065	0.0065	0.0065	0.0065	0.0065	0.0065
9	0.0034	0.0034	0.0034	0.0034	0.0034	0.0034	0.0034	0.0034	0.0034	0.0034
10	0.0022	0.0022	0.0022	0.0022	0.0022	0.0022	0.0022	0.0022	0.0022	0.0022

The input scans are preprocessed in SPM12 for co registration, motion correction, slice time correction , Normalization and arranged as Y matrix as shown in table 1. Applying kSVD to Y results in sparse dictionary for optimum value of k-6. The activations projected in fig 2. implies that, before acupuncture on the specified acu points , the more voxels are seen in sensory motor cortex. After the acu point pressure, the region is equivalent to a healthy subject activation. Few highlights are also seen in fig 2. Which states that the activation may be due to hearing during experiment paradigm, lateral unwanted thinking, some expectations or disappointments , fear. With 30 iterations , the leaning is considerable for K=6. If the K value is above or below this, provides deviation in activation.

4. CONCLUSION

The acu point **LI 11,GB 34** activation on a shaky hand subject is analysed and the functional localization on the block paradigm using kSVD is obtained. Our fMRI study confirmed that acupuncture at these two point can activate certain cognitive-related regions in shaky hands patients. These results also explain methodology in acupuncture research. The future direction is to classify the healthy controls and ET subjects using the identified spatial map and time series. The only demerit is the deactivations could not be accountable.

ACKNOWLEDGEMENT

The Authors would like to thank Scan center for having generously provided the Task and Rest fMRI scans for the particular study and for the cooperation in executing the acupuncture fMRI paradigm.

REFERENCES

1. Wei Qin, Jie Tian, Lijun Bai, Xiaohong Pan, Lin Yang, Peng Chen⁵, Jianping Dai, Lin Ai, Baixiao Zhao, Qiyong Gong, Wei Wang, Karen M von Deneen⁹ and Yijun Liu, **fMRI connectivity analysis of acupuncture effects on an amygdala-associated brain network**, *Molecular Pain* 2008 , 4:55 , ISSN:1744-8069.
2. Wenjing Huang et. al , **Characterizing Acupuncture stimuli using Brain Imaging with fMRI-Asystematic Review and Meta –Analysis of the Literature** , *PLOS One* Vol.7, Issue 4, April 2012.
3. Jinbo Sun, Yuanqiang Zhu, Lingmin Jin, Yang Yang, Karen M. von Deneen, Wei Qin, Qiyong Gong, and Jie Tian , **Partly Separated Activations in the Spatial distribution between de-qi and Sharp Pain during Acupuncture Stimulation: an fMRI-Based Study**, *Evidence-Based Complementary and Alternative Medicine* Volume 2012.
4. Yi Zhang et, al, **An fMRI study of acupuncture using independent component analysis**, *Neuroscience Letters*, Volume 449, Issue 1, January 2009, Pages 6–9.
5. Peng Liua, , **The hybrid GLM–ICA investigation on the neural mechanism of acupoint ST36: An fMRI study**, *Neuroscience Letters*, Volume 479, Issue 3, 2 August 2010, Pages 267–271.
6. Kong J, Ma L, Gollub RL, Wei J, Yang X, Li D, Weng X, Jia F, Wang C, Li F: **A Pilot Study of Functional Magnetic Resonance Imaging of the Brain During Manual and Electroacupuncture Stimulation of Acupuncture Point (LI-4 Hegu) in Normal Subjects Reveals Differential Brain Activation Between Methods**. *Journal of Alternate Complement Medicine*, 2002, 8(4):411-419.
7. K. Friston, J. Ashburner, S. Kiebel, T. Nichols, and W. E. Penny, **Statistical Parametric Mapping: The Analysis of Functional Brain Images**, New York: Academic, 2006.
8. M. Aharon, M. Elad, and A. Bruckstein, “**K-SVD: An algorithm for designing overcomplete dictionaries for sparse representation**,” *IEEE Trans. Signal Process.*, vol. 54, no. 11, p. 4311, Nov. 2006.
9. Kangjoo Lee, Sungho Tak, and Jong Chul Ye* “**A Data-Driven Sparse GLM for fMRI Analysis Using Sparse Dictionary Learning With MDL Criterion**”, *IEEE Transactions on Medical Imaging*, vol. 30, no. 5, may 2011.